

# A strategy for the identification of protein architectures directly from ion mobility mass spectrometry data reveals stabilizing subunit interactions in light harvesting complexes

Margit Kaldmäe,<sup>1</sup> Cagla Sahin,<sup>1</sup> Mihkel Saluri,<sup>2</sup> Erik G. Marklund ,<sup>3\*</sup> and Michael Landreh <sup>1\*</sup>

<sup>1</sup>Science for Life Laboratory, Department of Microbiology, Tumour and Cell Biology, Karolinska Institutet, Tomtebodavägen 23A, SE-171 65, Stockholm, Sweden

<sup>2</sup>School of Natural Sciences and Health, Tallinn University, Narva mnt 25, 10120, Tallinn, Estonia

<sup>3</sup>Department of Chemistry – BMC, Uppsala University, Box 576, SE-751 23, Uppsala, Sweden

Received 6 December 2018; Accepted 28 March 2019

DOI: 10.1002/pro.3609

Published online 19 April 2019 [proteinscience.org](http://proteinscience.org)

**Abstract:** Biotechnological applications of protein complexes require detailed information about their structure and composition, which can be challenging to obtain for proteins from natural sources. Prominent examples are the ring-shaped phycoerythrin (PE) and phycocyanin (PC) complexes isolated from the light-harvesting antennae of red algae and cyanobacteria. Despite their widespread use as fluorescent probes in biotechnology and medicine, the structures and interactions of their noncrystallizable central subunits are largely unknown. Here, we employ ion mobility mass spectrometry to reveal varying stabilities of the PC and PE complexes and identify their closest architectural homologues among all protein assemblies in the Protein Data Bank (PDB). Our results suggest that the central subunits of PC and PE complexes, although absent from the crystal structures, may be crucial for their stability, and thus of unexpected importance for their biotechnological applications.

**Keywords:** structural mass spectrometry; protein interactions; collision cross sections; protein complex stability; ion mobility; red algae

## Introduction

Phycobilisomes are large (up to 20 MDa) light-harvesting complexes found mainly in red algae and cyanobacteria.<sup>1</sup>

Their main components are ring-shaped heteromeric phycobiliprotein complexes composed of an equal number of  $\alpha$ - and  $\beta$ -subunits that each contain multiple

---

*Abbreviations:* APC, allophycocyanin; IM-MS, ion mobility mass spectrometry; PC, phycocyanin; PE, phycoerythrin; CCS, collision cross section.

Additional Supporting Information may be found in the online version of this article.

Grant sponsor: Karolinska Institutet Faculty-Funded Career Grant StratNeuro Start-up grant; Grant sponsor: Vetenskapsrådet Marie Skłodowska Curie International Career Grant; Grant sponsor: Swedish Research Council 2013\_08807 2015-00559; Grant sponsor: European Commission; Grant sponsor: Swedish Foundation for Strategic Research.

\*Correspondence to: Erik G. Marklund, Department of Chemistry – BMC, Uppsala University, Box 576, SE-751 23 Uppsala, Sweden. E-mail: [erik.marklund@kemi.uu.se](mailto:erik.marklund@kemi.uu.se); Michael Landreh, Science for Life Laboratory, Department of Microbiology, Tumour and Cell Biology, Karolinska Institute, Tomtebodavägen 23A, SE-171 65 Stockholm, Sweden. E-mail: [michael.landreh@ki.se](mailto:michael.landreh@ki.se)

This is an open access article under the terms of the Creative Commons Attribution-NonCommercial License, which permits use, distribution and reproduction in any medium, provided the original work is properly cited and is not used for commercial purposes.

tetrapyrrole chromophores.<sup>2</sup> These complexes are grouped into the pink phycoerythrins (PE) and the blue phycocyanins (PC), as well as the blue allophycocyanin (APC). They are among the brightest fluorescent molecules known, and have therefore numerous applications as probes in biotechnology, food coloring additives, and even anticancer agents.<sup>3,4</sup> Although recombinant production has been explored, their purification from natural sources has remained the production standard for all applications.<sup>5–7</sup> As a result, there is a significant effort to find new species of red algae for the extraction of phycobiliproteins with different properties, and methods that enable reliable characterization of their structure and integrity are in high demand.<sup>8,9</sup>

In the native algal phycobilisome, PC and PE rings are assembled into rods and connected to a central APC core with the help of a heterogeneous family of linker polypeptides. PE and PC interact with a number of linker proteins, including one occupying the central cavity of the ring. PE commonly co-purifies with its central linker, referred to as the  $\gamma$ -subunit, as an  $\alpha_6\beta_6\gamma$  complex (Fig. 1). This  $\gamma$ -subunit is seen in the center of the  $\alpha_6\beta_6$  ring as a diffuse electron density in high-resolution structures.<sup>10,11</sup> PC is known to associate with a central linker protein similar to the  $\gamma$ -subunit in PE, but again, detailed crystallographic evidence for the interaction is lacking.<sup>12</sup> The structure of the complex between PE and PC and their  $\gamma$ -subunits remains unsolvable in crystallography because it lacks the symmetry of the  $\alpha_6\beta_6$  ring, which yields rotational averaging of its electron density.

We therefore turned to mass spectrometry (MS) as an alternative strategy to assess the structural integrity of PE and PC complexes with their central linker subunits. Here, protein complexes can be gently transferred from near-physiological solutions to the gas phase, often without significant distortions of their native structures

or interactions. This enables us to determine the masses and abundances of intact complexes, or their individual components following dissociation inside the mass spectrometer.<sup>13,14</sup> In combination with ion mobility (IM) measurements, the approach can provide information about their overall structure and connectivity.<sup>15</sup> Since MS has been used to monitor pH and concentration effects on the assembly light-harvesting complexes,<sup>16,17</sup> we expect IM-MS to be able to unravel the architectures of native phycobiliprotein assemblies.

## Results and Discussion

As first step, we analyzed the stoichiometry of PE by MS. Using instrumental conditions optimized for the transfer of intact protein complexes to the gas phase,<sup>18</sup> we obtained well-resolved spectra of PE with no signs of complex dissociation [Fig. 2(a)]. The spectra show two overlapping series of peaks with narrow charge state distributions centered around the 35+ ions, indicating non-denatured conformations.<sup>19</sup> The masses of  $262,279 \pm 65$  and  $265,964 \pm 108$  Da are both in good agreement with  $\alpha_6\beta_6\gamma$  complexes (Table S1). Leney et al. found that PE may adopt variable stoichiometries with 5 and 7  $\alpha$ - and  $\beta$ -subunits.<sup>16</sup> However, this does not explain the 3.6 kDa difference between the two populations observed here. Instead, SDS-polyacrylamide gel electrophoresis (PAGE) analysis clearly shows the presence of two different  $\gamma$ -subunits separated by less than 5 kDa (Fig. S1). Similar observations were previously interpreted as PE containing two  $\gamma$ -subunits per complex.<sup>20</sup> Our results on the other hand clearly show that purified PE exists as  $\alpha_6\beta_6\gamma$  complexes with either a 28- ( $\gamma'$ ) or a 32-kDa subunit ( $\gamma''$ ). The different  $\gamma$ -subunits likely distinguish PE from the distal or middle regions of the light-harvesting rod.<sup>21</sup> In addition, a

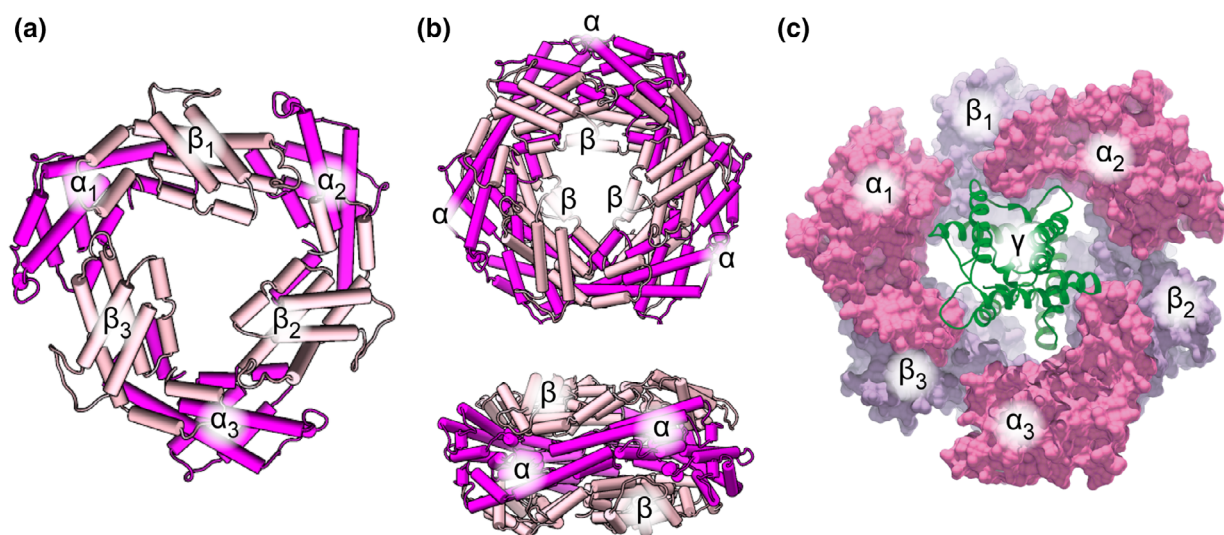


**Figure 1.** Architecture of the  $\alpha_6\beta_6\gamma$  PE complex. (a) The basic unit of the PE complex is a ring-shaped trimer composed of three  $\alpha\beta$  dimers.  $\alpha$ - and  $\beta$ -subunits are rendered in magenta and pink, respectively. (b) The  $\alpha$ -subunits of two  $\alpha_3\beta_3$  trimers stack together to form the  $\alpha_6\beta_6$  ring, shown as top and side view. (c) The ring cavity is occupied by the  $\gamma$ -subunit (green), shown here based on an individual PE complex from the cryo-EM structure of the entire phycobilisome (PDB ID 5Y6P) with the top  $\alpha_3\beta_3$  trimer removed.

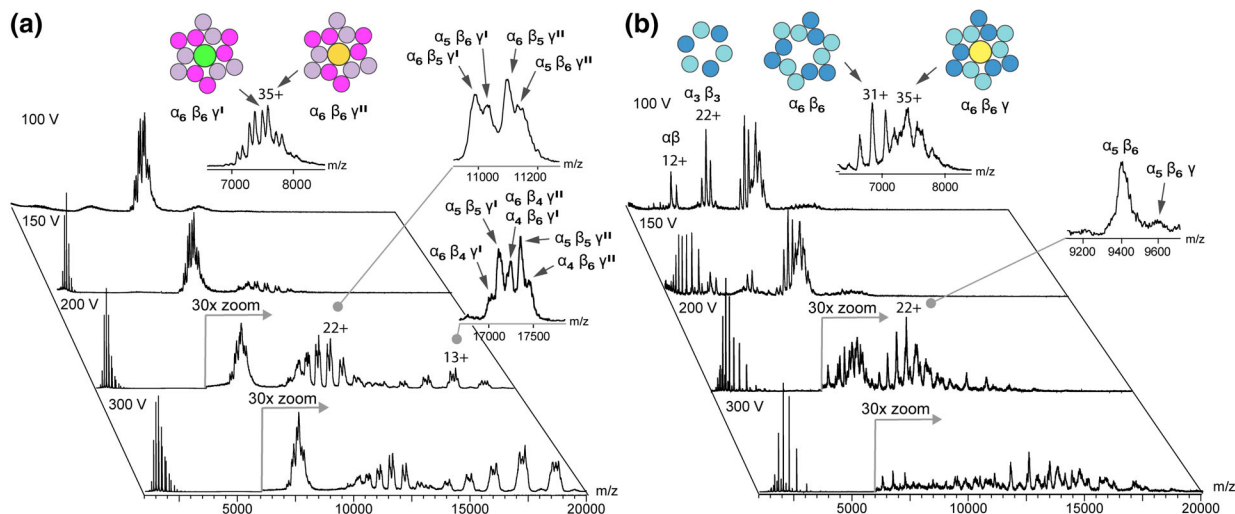


**Figure 2.** Mass spectrometric analysis of PE and PC. (a) Intact mass and gas-phase dissociation of PE. At low cone voltages, PE exhibits a homogeneous  $\alpha_6\beta_6\gamma$  stoichiometry containing either a 28 or 32 kDa  $\gamma$ -subunits ( $\gamma'$  or  $\gamma''$ ). Increasing the cone voltage releases  $\alpha_6\beta_6\gamma$  and subsequently  $\alpha_5\beta_5\gamma$  sub-complexes, but cannot dissociate all  $\alpha_6\beta_6\gamma$  assemblies. (b) Intact mass and gas-phase dissociation of PC. Under gentle ionization conditions, MS shows the presence of PC complexes with and without a  $\gamma$ -subunit. Raising the cone voltage induces dissociation of both species, with the  $\alpha_6\beta_6$  and the  $\alpha_6\beta_6\gamma$  complexes fully dissociated at 200 and 300 V, respectively.

minor population of  $(\alpha_6\beta_6\gamma)_2$  dimers with 55+ charges can be detected; however, their  $\gamma$ -composition could not be resolved (Fig. S2a).

Next, we subjected the intact PE complexes to gas-phase dissociation, which provides information about subunit connectivity and stability. By raising the voltage of the sample cone at the entrance to the vacuum region of the mass spectrometer, the desolvated protein assemblies are accelerated and undergo dissociation via collisions with residual gas molecules prior to MS analysis. Upon increasing the cone voltage to 150 V, additional peaks corresponding to free  $\beta$ -subunits and  $\alpha_6\beta_5\gamma$  complexes were detected, indicating that the  $\beta$ -subunit interactions are the most easily disrupted ones [Fig. 2(a), Figs. S2b, S3]. When the cone voltage is increased further, a second fragment series corresponding to PE complexes that have lost another subunit can be observed, although a significant amount of intact  $\alpha_6\beta_6\gamma$  persists. Notably, PE with  $\gamma'$ - or  $\gamma''$ -subunits exhibited the same fragment peak intensities, suggesting similar gas-phase stabilities irrespective of which  $\gamma$ -subunit is present (Fig. S1b). Taken together, the fragmentation pattern indicates that for the PE complex investigated here,  $\beta$ -subunits dissociate first, followed by dissociation of an  $\alpha$ - or a second  $\beta$ -subunit from the core containing the  $\gamma$ -subunit.

Having established the oligomeric state and dissociation behavior of PE, we then employed the same MS approach to investigate PC, whose fold and assembly are near-identical to that of PE. However, to our surprise, mass spectra of PC recorded using gentle ionization conditions did not show uniform oligomers like PE, but four series of peaks [Fig. 2(b)]. Based on their masses, we identified them as  $\alpha\beta$ -heterodimers ( $37,526 \pm 56$  Da),  $\alpha_3\beta_3$ -heterohexamers ( $112,456 \pm 48$  Da), the complete  $\alpha_6\beta_6$ -assembly ( $225,280 \pm 79$  Da), and a complex

corresponding to the  $\alpha_6\beta_6$ -ring with an additional 33 kDa component similar to the intact  $\alpha_6\beta_6\gamma$  PE complex ( $259,135 \pm 199$  Da) (Table S1). We observe that the presence of the linker protein causes significant peak broadening, suggesting that the extra subunit may be more heterogeneous than the  $\alpha$ - and  $\beta$ -units. The main charge states are 12+ for  $\alpha\beta$ , 22+ for  $\alpha_3\beta_3$ , and 31+ for  $\alpha_6\beta_6$ . Since the charges of all dissociation products have to add up to the charge for the parent ion, the  $\alpha\beta$  and  $\alpha_3\beta_3$  populations cannot arise from gas-phase dissociation of the intact  $\alpha_6\beta_6$  complex, but likely exist in solution. In addition, we detected minor populations of  $(\alpha_6\beta_6)_2$  and  $(\alpha_6\beta_6\gamma)_2$  dimers, which may arise from concentration-dependent self-association (Fig. S2a). Together, these findings provide clear evidence that PC, unlike PE, can exist as a  $\alpha_6\beta_6$  complex without retaining a linker protein as  $\gamma$ -subunit. At the same time, our spectra show that a significant proportion of the PC complexes retain a phycobilisomal linker protein, which we here refer to as PC  $\gamma$ -subunit in analogy to the linker in the intact PE complex.

When subjected to gas-phase dissociation, the PC investigated here predominantly releases  $\alpha$ -, not  $\beta$ -subunits, resulting in a mixture of low-intensity populations including  $\alpha_5\beta_6$  and  $\alpha_5\beta_6\gamma$  complexes [Fig. 2(b), Fig. S2c]. Notably, at 200 V, the  $\alpha_6\beta_6$  complexes had readily dissociated, as had the  $\alpha_6\beta_6\gamma$  complex at 300 V. Together, the observations suggest that PC has a lower resilience to gas-phase dissociation than PE, which is even further reduced in the absence of the  $\gamma$ -subunit.

In the phycobilisome, the linker protein scaffold connects the PE and PC rods to central  $\alpha_3\beta_3$  rings of APC.<sup>1</sup> We therefore extended our MS analysis to APC to investigate whether this complex, like PE and PC, can retain linker proteins. However, no additional subunits except for APC-specific  $\alpha$  and  $\beta$  were observed, and the

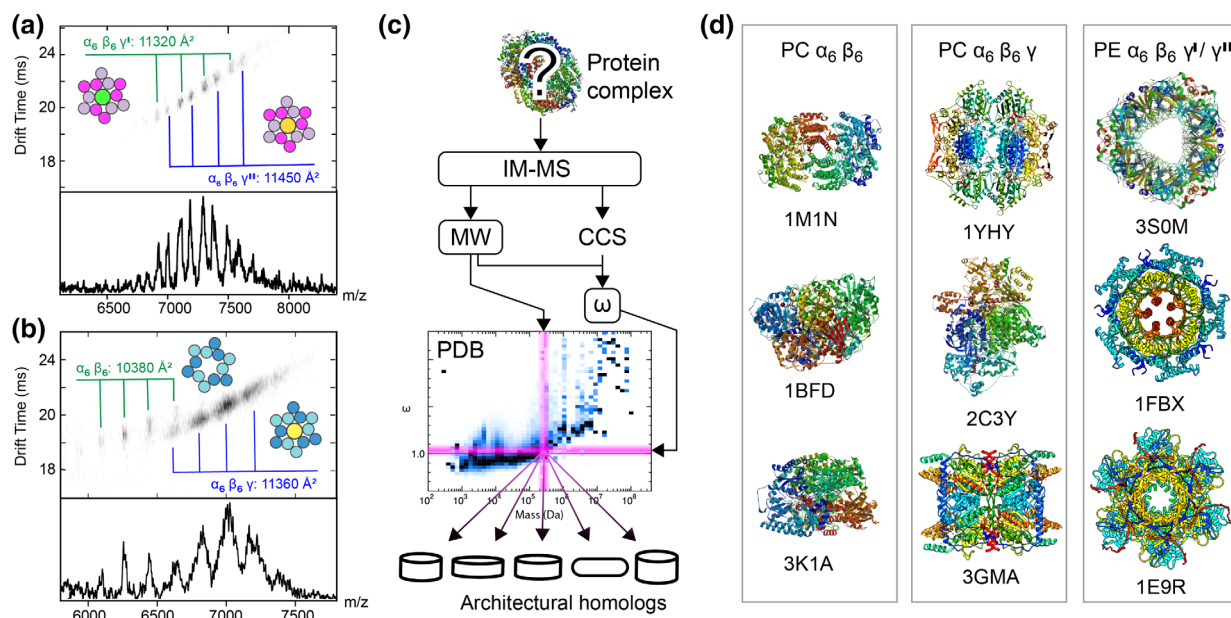


**Figure 3.** Using IM-MS data to mine the known structural proteome distinguishes ring-like architectures and structural collapse in the absence of specific reference structures. (a, b) Mobiligrams of the intact PE and PC complexes show narrow arrival time distributions. The average CCS values for each ion series are indicated. (c) Illustration of the IM-MS-based PDB search strategy. (d) The structures of the top three architectural homologues identified based on the molecular weights and experimental CCSs of PC and PE complexes reveal that  $\alpha_6\beta_6\gamma'$  and  $\alpha_6\beta_6\gamma''$  PE retain their ring architectures, while  $\alpha_6\beta_6\gamma$  PC undergoes partial collapse and  $\alpha_6\beta_6$  PC complete structural collapse.

$\alpha_3\beta_3$  complex fully dissociated at 200 V (Fig. S4). We therefore conclude that retention of the linker subunits is not due to their overall abundance in the phycobilisome, but specific to PE and PC.

Since we found that PE and PC, despite their near-identical ring structures, differ significantly in their  $\gamma$ -subunit interactions, we asked how these interactions affect the overall architecture of the complexes. To answer this question, we employed IM-MS, which informs about the shape of ions by measuring their drift time through an inert buffer gas under the influence of a weak electric field. Long and short drift times indicate loosely packed or compact shapes, respectively. The influence of an ion's structure is contained in its collision cross section (CCS), which can be inferred from the drift time, the ion's net charge, and the instrument parameters. The CCS is a measure to how much of the protein is exposed for collisions with the buffer gas, and like the drift time, it decreases with the ion's compactness.<sup>22</sup>

We determined the CCS values (Table S2) of PE to be 11,320 Å<sup>2</sup> for  $\alpha_6\beta_6\gamma'$  and 11,450 Å<sup>2</sup> for  $\alpha_6\beta_6\gamma''$ , with a standard deviation of less than 50 Å<sup>2</sup> between all charge states [Fig. 3(a)]. PC gave a CCS of 11,360 ± 42 Å<sup>2</sup> for the  $\alpha_6\beta_6\gamma$  complex and 10,380 ± 242 Å<sup>2</sup> for the  $\alpha_6\beta_6$  ring, with 10,047 Å<sup>2</sup> for the lowest charge being more than 10% below the values for the complexes containing  $\gamma$ -subunits [Fig. 3(b)]. Since no crystal structure of an intact  $\alpha_6\beta_6\gamma$  complex of PE or PC has been reported, we calculated the theoretical CCS for the crystal structures without  $\gamma$ -subunits as 11,369 Å<sup>2</sup> for algal PE (PDB ID

1L1A) and 11,286 Å<sup>2</sup> for PC (PDB ID 1GHO). These values are in good agreement with the CCSs determined for the  $\alpha_6\beta_6\gamma$  complexes, but significantly higher than that measured for  $\alpha_6\beta_6$  PC. However, in the absence of a matching reference structure, it was not possible to determine whether the presence of the  $\gamma$ -subunit increases the CCS by protruding from the complex or stabilizing its overall architecture against compaction in the gas phase. We therefore reasoned that the combination of molecular weight and experimental CCS might constitute a signature for complexes with certain architectures. Because the theoretical CCSs have already been computed for all biological assemblies in the PDB,<sup>23</sup> we could use a protein's experimental mass and CCS to identify the nearest neighbors within the known structural proteome [Fig. 3(c)]. To test this approach, we first used the mass of PE dodecamer together with the calculated CCS and noted that the majority of neighbors were ring-shaped (Fig. S5). Another few were otherwise hollow, and yet another few had other architectures. Having demonstrated the feasibility of the search strategy, we used the values for  $\alpha_6\beta_6\gamma'$  and  $\alpha_6\beta_6\gamma''$  PE, which strikingly returned mostly ring- or disc-shaped complexes among the structural homologues, with a large overlap between the two sets. A selection made using the CCS and molecular weight of  $\alpha_6\beta_6\gamma$  PC also contained rings and more extended architectures, while  $\alpha_6\beta_6$  PC, on the other hand, identified exclusively globular protein complexes [Fig. 3 (d)]. These observations suggest that PE is able to retain its solution structure in the gas phase, while PC with its  $\gamma$ -subunit may undergo partial collapse, and without

$\gamma$ -subunit total collapse. PC therefore exhibits similar behavior as other labile ring-shaped complexes, which easily rearrange into more compact shapes when subjected to desolvation and collisional activation.<sup>24,25</sup>

Our observations from IM-MS are in striking agreement with the relative gas-phase stabilities of both complexes (Fig. 2), indicating that the central linker protein in PC provides overall less structural support of the ring than that in PE. Furthermore, we find that using IM-MS data to mine the PDB makes it possible to identify likely complex architectures without a need for theoretical CCS calculations of generated candidate structure models. Hence, it enables us to directly assess their structural integrity for, for example, biotechnological applications.

## Conclusions

Numerous studies have demonstrated functional roles for the linker proteins that form the  $\gamma$ -subunits in PE- and PC, most notably as regulators of different conformational states and fluorescence properties.<sup>12,26</sup> Therefore, preserving  $\gamma$ -subunit interactions in phycobiliprotein complexes, particularly their less stable association with PC, is likely crucial for maintaining their desired spectroscopic properties. The possibilities offered by native MS to assess integrity and composition of phycobiliproteins as demonstrated here are evident, considering the widespread applications of phycobiliproteins as fluorescent probes in biotechnology, and particularly the continued efforts to find new natural sources.

Perhaps most importantly, we show that IM-MS data can be used to directly determine the effects of the  $\gamma$ -subunits on the overall architecture of the different phycobiliprotein complexes without a need for a specific reference structure. Although the present approach would be less well-suited for complexes with more globular structures, which may give only subtle differences in their CCS-MW relation, or complexes with unique architectures without close structural homologues in the PDB, it has considerable potential for the analysis of protein complexes without prior structural information. More generally, the use of IM-MS data to find related structures in the PDB can provide classification of unknown protein complexes beyond biotechnological applications, adding another dimension to MS-driven protein structure analyses.

## Materials and Methods

### Protein preparation

Phycocyanin (Cat. number 52468), R-phycoerythrin (Cat. number 52412), and APC (Cat. number A7472) were purchased from Sigma. Proteins were dissolved in PBS to a final concentration of approximately 0.2 mg/mL, corresponding to about 2  $\mu$ M. For MS analysis, proteins were buffer-exchanged into 1 M

ammonium acetate, pH 7.5, using Biospin 6 microcentrifuge columns (BioRad, CA).

### Mass spectrometry

Mass spectra were acquired on a Micromass LCT ToF modified for analysis of intact protein complexes (MS Vision, The Netherlands) equipped with an off-line nanospray source. Samples were introduced via coated borosilicate capillaries (Thermo Scientific, Germany). The capillary voltage was 1.5 kV. Collisional activation was performed by ramping the cone voltage between 100 and 300 V. The radio frequency (RF) lens voltage was 1.5 kV. The source pressure was maintained at 9.0 mbar to prevent in-source dissociation. The mass scale was calibrated using cesium iodide.

Ion mobility MS spectra were acquired on a Synapt G2S travelling wave ion mobility mass spectrometry (TWIMS) MS equipped with an offline nanospray source. The capillary voltage was 1.5 kV and the source temperature was maintained at 120°C and the sample cone at 80 V. The pressures were as follows: backing 3.29 mbar, source  $5.8 \times 10^{-3}$  mbar, trap  $4.41 \times 10^{-2}$  mbar, and IMS 4.16 mbar. The ion mobility spectrometry (IMS) settings were as follows: wave height 20 V and wave velocity 550 m/s. The drift gas was nitrogen with a flow rate of 50 mL/min and the collision voltages in the ion trap and transfer were 5 and 2 V, respectively. The trap DC bias was 45 V and the IMS DC bias was 3 V. TWIMS calibration was performed using the 33+ to 37+ charge states of pyruvate kinase as sole calibrant, since it very closely matches the molecular weight and average charge as intact PE and PC.<sup>27</sup> Data were analyzed using the MassLynx 4.1 and PULSAR (pulsar.chem.ox.ac.uk<sup>28</sup>) software packages. Average masses and standard deviations between charge states were determined using a Microsoft Excel file kindly provided by the Benesch Laboratory, University of Oxford.

### Structure analysis

For theoretical CCS calculations, crystal structures of  $\alpha_6\beta_6$  PE (PDB ID 1LIA) and PC (PDB ID 1GHO) were used. Theoretical trajectory-method-corrected CCS values for the  $\alpha_6\beta_6$  complexes of PE and PC were determined by averaging 10 separate calculations using IMPACT (impact.chem.ox.ac.uk).<sup>23</sup> Protein structures were visualized and edited using UCSF Chimera.<sup>29</sup>

### CCS-mass-based modeling using IMPACT

Masses and CCSs were used as input to the python script find\_omega\_neighbours.py, which is distributed alongside IMPACT<sup>23</sup>, with default parameters. In the script, the CCSs are converted to reduced cross-sections ( $\omega$ ), where a  $\omega$  above (or below) 1.0 signifies a higher (or lower) CCS than expected for a protein of the given mass (see Reference 23). The script returns the 10 protein complexes that best match the target mass and  $\omega$ , and consequently, the CCS. The script was run using (i) the CCS inferred from the trimmed structure model of the PE  $\alpha_6\beta_6$  together with the expected mass calculated from

the masses of its monomers, (ii) the experimental data for the PE  $\alpha_6\beta_6\gamma'$  and  $\alpha_6\beta_6\gamma''$  complexes, (iii) the experimental data for the PC  $\alpha_6\beta_6\gamma$  complex, and (iv) the experimental data for the PC  $\alpha_6\beta_6$  complex.

### Fluorescence measurements

Fluorescence spectra of 2  $\mu\text{M}$  PE or PC in PBS with 0–5% formic acid were recorded on a Tecan Spark 20 M multimode reader (Tecan Instruments, Switzerland) using Corning COSTAR black flat bottom 96-well plates (Sigma-Aldrich, Germany). For PE, excitation wavelength was 530 nm; emission was recorded between 550 and 750 nm in 1 nm steps with 5 nm bandwidth and an integration time of 40  $\mu\text{s}$ . For PC, excitation wavelength was 595 nm; emission was recorded between 630 and 750 nm in 1 nm steps with 5 nm bandwidth and an integration time of 40  $\mu\text{s}$ . Data were visualized using the Magellan software package (Tecan Instruments, Switzerland).

### Acknowledgments

The authors would like to extend special thanks to Nicklas Österlund and Prof. Leopold Ilag, Stockholm University, for access to the Synapt G2S IM-MS instrument, and to Prof. Dame Carol Robinson and Prof. Justin Benesch, University of Oxford, for encouragement and helpful discussions. M.L. gratefully acknowledges technical support from MS Vision, NL. M.L. is supported by an Ingvar Carlsson Award from the Swedish Foundation for Strategic Research, a KI faculty-funded Career Position, and a KI-StratNeuro starting grant. E.G.M. holds a Marie Skłodowska Curie International Career Grant from the European Commission and the Swedish Research Council (2015-00559). Special thanks to Prof. Sir David P. Lane, Karolinska Institutet, for support through Swedish Research Council Grant 2013\_08807.

### References

1. Watanabe M, Ikeuchi M (2013) Phycobilisome: architecture of a light-harvesting supercomplex. *Photosynth Res* 116:265–276.
2. Adir N (2005) Elucidation of the molecular structures of components of the phycobilisome: reconstructing a giant. *Photosynth Res* 85:15–32.
3. Wan DH, Zheng BY, Ke MR, Duan JY, Zheng YQ, Yeh CK, Huang JD (2017) C-Phycocyanin as a tumour-associated macrophage-targeted photosensitizer and a vehicle of phthalocyanine for enhanced photodynamic therapy. *Chem Commun* 53:4112–4115.
4. Klein B, Buchholz R. Microalgae as sources of food ingredients and nutraceuticals, (2013) *Microbial production of food ingredients, enzymes and nutraceuticals*, Amsterdam, NL: Elsevier, pp 559–570.
5. Eriksen NT (2008) Production of phycocyanin - a pigment with applications in biology, biotechnology, foods and medicine. *Appl Microbiol Biotechnol* 80:1–14.
6. Guan X, Qin S, Su Z, Zhao F, Ge B, Li F, Tang X (2007) Combinational biosynthesis of a fluorescent cyanobacterial holo- $\alpha$ -phycocyanin in *Escherichia coli* by using one expression vector. *Appl Biochem Biotechnol* 142:52–59.
7. Cuellar-Bermudez SP, Aguilar-Hernandez I, Cardenas-Chavez DL, Ornelas-Soto N, Romero-Ogawa MA, Parra-Saldivar R (2015) Extraction and purification of high-value metabolites from microalgae: essential lipids, astaxanthin and phycobiliproteins. *J Microbiol Biotechnol* 8:190–209.
8. Sonani RR (2016) Recent advances in production, purification and applications of phycobiliproteins. *World J Biol Chem* 7:100–109.
9. Dumay J, Morancais M, Munier M, Le Guillard C, Fleurence J (2014) Phycoerythrins: Valuable proteinic pigments in red seaweeds. *Adv Bot Res* 71:321–343.
10. Chang WR, Jiang T, Wan ZL, Zhang JP, Yang ZX, Liang DC (1996) Crystal structure of R-phycoerythrin from *Polysiphonia urceolata* at 2.8 Å resolution. *J Mol Biol* 262:721–731.
11. Ritter S, Hiller RG, Wrench PM, Welte W, Diederichs K (1999) Crystal structure of a phycourobilin-containing phycoerythrin at 1.90-Å resolution. *J Struct Biol* 126:86–97.
12. David L, Marx A, Adir N (2011) High-resolution crystal structures of trimeric and rod phycocyanin. *J Mol Biol* 405:201–213.
13. Benesch JL, Robinson CV (2006) Mass spectrometry of macromolecular assemblies: preservation and dissociation. *Curr Opin Struct Biol* 16:245–251.
14. Lssl P, van de Waterbeemd M, Heck AJ (2016) The diverse and expanding role of mass spectrometry in structural and molecular biology. *EMBO J* 35:2634–2657.
15. Ben-Nissan G, Sharon M (2018) The application of ion-mobility mass spectrometry for structure/function investigation of protein complexes. *Curr Opin Chem Biol* 42:25–33.
16. Leney AC, Tschanz A, Heck AJR (2018) Connecting color with assembly in the fluorescent B-phycoerythrin protein complex. *FEBS J* 285:178–187.
17. Eisenberg I, Harris D, Levi-Kalisman Y, Yochelis S, Shemesh A, Ben-Nissan G, Sharon M, Raviv U, Adir N, Keren N, Paltiel Y (2017) Concentration-based self-assembly of phycocyanin. *Photosynth Res* 134:39–49.
18. Sobott F, Hernndez H, McCammon MG, Tito MA, Robinson CV (2002) A tandem mass spectrometer for improved transmission and analysis of large macromolecular assemblies. *Anal Chem* 74:1402–1407.
19. Hall Z, Robinson CV (2012) Do charge state signatures guarantee protein conformations? *J Am Soc Mass Spectrom* 23:1161–1168.
20. Wang L, Wang S, Fu X, Sun L (2015) Characteristics of an R-phycoerythrin with two  $\gamma$  subunits prepared from red macroalga *Polysiphonia urceolata*. *PLoS One* 10:e0120333.
21. Zhang J, Ma J, Liu D, Qin S, Sun S, Zhao J, Sui SF (2017) Structure of phycobilisome from the red alga *Griffithsia pacifica*. *Nature* 551:57–63.
22. Marklund EG (2015) Molecular self-occlusion as a means for accelerating collision cross-section calculations. *Int J Mass Spectrom* 386:54–55.
23. Marklund EG, Degiacomi MT, Robinson CV, Baldwin AJ, Benesch JLP (2015) Collision cross sections for structural proteomics. *Structure* 23:791–799.
24. Ruotolo BT, Giles K, Campuzano I, Sandercock AM, Bateman RH, Robinson CV (2005) Biochemistry: evidence for macromolecular protein rings in the absence of bulk water. *Science* 310:1658–1661.
25. Hall Z, Politis A, Bush MF, Smith LJ, Robinson CV (2012) Charge-state dependent compaction and dissociation of protein complexes: insights from ion mobility and molecular dynamics. *J Am Chem Soc* 134:3429–3438.
26. Gwizdala M, Krger TPJ, Wahadoszamen M, Gruber JM, Van Grondelle R (2018) Phycocyanin: one complex, two states, two functions. *J Phys Chem Lett* 9:1365–1371.

27. Bush MF, Hall Z, Giles K, Hoyes J, Robinson CV, Ruotolo BT (2010) Collision cross sections of proteins and their complexes: a calibration framework and database for gas-phase structural biology. *Anal Chem* 82:9557–9565.
28. Allison TM, Reading E, Liko I, Baldwin AJ, Laganowsky A, Robinson CV (2015) Quantifying the stabilizing effects of protein–ligand interactions in the gas phase. *Nat Commun* 6:8551.
29. Pettersen EF, Goddard TD, Huang CC, Couch GS, Greenblatt DM, Meng EC, Ferrin TE (2004) UCSF chimera—a visualization system for exploratory research and analysis. *J Comput Chem* 25:1605–1612.